Therapeutics, Targets, and Chemical Biology

Cancer Research

RK-33 Radiosensitizes Prostate Cancer Cells by Blocking the RNA Helicase DDX3

Min Xie[1], Farhad Vesuna[1], Saritha Tantravedi[1], Guus M. Bol[1,2], Marise R. Heerma van Voss[1,2], Katriana Nugent[3], Reem Malek[3], Kathleen Gabrielson[4,5], Paul J. van Diest[2], Phuoc T. Tran[3], and Venu Raman[1,2,6]

Abstract

Despite advances in diagnosis and treatment, prostate cancer is the most prevalent cancer in males and the second highest cause of cancer-related mortality. We identified an RNA helicase gene, *DDX3* (DDX3X), which is overexpressed in prostate cancers, and whose expression is directly correlated with high Gleason scores. Knockdown of DDX3 in the aggressive prostate cancer cell lines DU145 and 22Rv1 resulted in significantly reduced clonogenicity. To target DDX3, we rationally designed a small molecule, RK-33, which docks into the ATP-binding domain of DDX3. Functional studies indicated that RK-33 preferentially bound to DDX3 and perturbed its activity. RK-33 treatment of prostate cancer cell lines DU145, 22Rv1, and LNCaP (which have high DDX3 levels) decreased proliferation and induced a G_1 phase cell-cycle arrest. Conversely, the low DDX3–expressing cell line, PC3, exhibited few changes following RK-33 treatment. Importantly, combination studies using RK-33 and radiation exhibited synergistic effects both *in vitro* and in a xenograft model of prostate cancer demonstrating the role of RK-33 as a radiosensitizer. Taken together, these results indicate that blocking DDX3 by RK-33 in combination with radiation treatment is a viable option for treating locally advanced prostate cancer. *Cancer Res; 76(21); 6340–50. ©2016 AACR.*

Introduction

Prostate cancer is the most common noncutaneous malignant cancer in men in Western countries. Despite advances in diagnosis and treatment, prostate cancer still remains the most prevalent cancer in males, with an estimated 180,890 new cases and 26,120 deaths in the United States in 2016 (1). It has been suggested that the development of prostate cancer from benign prostatic epithelial cells is a stepwise progression that leads to high-grade prostatic intraepithelial neoplasia, invasive adenocarcinoma, distant metastatic disease, and finally lethal castration-resistant metastatic disease (2). Screening and treatment monitoring of prostate cancer utilizes mainly the highly sensitive and specific prostate-specific antigen (PSA) serum biomarker (3). However, there are many drawbacks to the use of PSA as a screening biomarker tool, including unnecessary biopsies and low specificity. Furthermore, PSA has limitations as a prognostic and predictive biomarker (4). Although there are reports of other biomarkers associated with prostate cancer patients, including but not limited to markers of apoptosis such as B-cell lymphoma 2 (BCL2) and BCL2-associated X protein, a marker of proliferation rate (Ki67), p53 mutation or expression, p27, E-cadherin, p16, and PTEN expression, none of these biomarkers have been prospectively validated. Thus, new prognostic biomarkers are required, especially to differentiate between low and high grades of aggressive cancer to improve clinical management (4, 5).

Recently, we have discovered that an RNA helicase, DDX3, is dysregulated in many cancer types, including prostate cancer. Our earlier investigations showed that overexpression of DDX3 induced an epithelial–mesenchymal transition, along with increased motility and invasive capabilities, in cigarette smoke-induced breast cancer (6). DDX3 also modulates cell adhesion and motility (7), and has an important role in the hypoxia response (8). DDX3 is a multifunctional protein that belongs to the aspartate-glutamate-alanine-aspartate (D-E-A-D) box RNA helicase family (9–11). The putative functions of DDX3 have been associated with a variety of cellular functions, including cell-cycle progression, cellular proliferation, and apoptosis under various conditions (12–15). On the basis of the crystallographic structure of DDX3, we rationally designed a small-molecule inhibitor, RK-33, which has been demonstrated to bind to DDX3 and inhibit its helicase activity in breast and lung cancer cell lines (6, 16–18). RK-33 inhibits proliferation of multiple lung cancer cell lines in a dose-dependent manner and acts as a radiosensitizer in lung cancer mice models (19).

[1]Department of Radiology and Radiological Science, Johns Hopkins University School of Medicine, Baltimore, Maryland. [2]Department of Pathology, University Medical Center Utrecht, Utrecht, the Netherlands. [3]Department of Radiation Oncology and Molecular Radiation Sciences, Johns Hopkins University School of Medicine, Baltimore, Maryland. [4]Department of Molecular and Comparative Pathobiology, Johns Hopkins University School of Medicine, Baltimore, Maryland. [5]Department of Pathology, Johns Hopkins University School of Medicine, Baltimore, Maryland. [6]Department of Oncology, Johns Hopkins University School of Medicine, Baltimore, Maryland.

Note: Supplementary data for this article are available at Cancer Research Online (http://cancerres.aacrjournals.org/).

M. Xie and F. Vesuna contributed equally to this article.

Corresponding Author: Venu Raman, Division of Cancer Imaging Research, Department of Radiology and Radiological Science, Johns Hopkins University School of Medicine, 720 Rutland Avenue, Traylor 340, Baltimore, MD 21205. Phone: 410-955-7492; Fax: 410-614-1948; E-mail: vraman2@jhmi.edu

doi: 10.1158/0008-5472.CAN-16-0440

AACR

Conventional treatments for prostate cancer include active surveillance, surgery, radiotherapy, and chemotherapy. Radiotherapy has been used effectively as the first-line treatment for locally advanced prostate cancer. However, radioresistance can develop in 14%–91% of patients after radiotherapy (20). A radiosensitizer, combined with radiotherapy, may provide not only the benefit of higher radiosensitivity, but may also allow radiation dose reduction to reduce normal tissue toxicity.

Here, we report that DDX3 expression levels correlate to the aggressiveness of prostate cancer cell lines and patient tumor samples. Knockdown of DDX3 leads to significantly reduced clonogenic ability in aggressive androgen-insensitive prostate cancer cell lines, such as DU145 and 22Rv1. Our rationally designed DDX3 inhibitor showed inhibition of cell proliferation in the high DDX3–expressing prostate cancer cell lines DU145, 22Rv1, and LNCaP, compared with little inhibition in the low DDX3–expressing cell line, PC3. Interestingly, combination studies using RK-33 and radiation exhibited synergistic effects both *in vitro* and in a xenograft model of prostate cancer. As radiation is a mainstay of high-grade prostate cancer treatment, we feel that the use of DDX3 may be used as a biomarker to select for RK-33 treatment, which in combination with radiation, will not only significantly increase local control, but also reduce many of the side effects associated with current conventional therapy.

Materials and Methods

Cell culture and reagents

PC3, 22Rv1, and DU145 cells were obtained from Dr. Phuoc Tran (The Johns Hopkins University, Baltimore, MD) in 2013. PC3 and 22Rv1 were authenticated by short tandem repeat profiling in 2015. DU145 was purchased from ATCC in 2013. LNCaP cells were obtained from Dr. Kenneth Pienta (The Johns Hopkins University) from ATCC in 2011. DU145-Luc cancer cells were kindly provided by Dr. Evan Keller (University of Michigan, Ann Arbor, MI) in 2014. Cells were maintained in RPMI1640 (Corning) containing 10% FBS. All cell lines were maintained under standard sterile cell culture conditions in a humidified incubator at 37°C and air containing 5% CO_2. The primary antibodies used were mAbs against DDX3 (21). DDX3 shRNA lentiviral constructs have been described previously (6). Wound-healing assays were performed as described previously (6). Cell proliferation and flow cytometry assays were carried out as described previously (22, 23).

Colony formation assays

PC3, DU145, and 22Rv1 cells transduced with vector and shDDX3 were seeded in 6-well plates at a density of 200 cells per well for PC3 and DU145, and 250 cells per well for 22Rv1. After incubation for 2–3 weeks, colonies were stained with 0.05% (w/v) crystal violet and counted. PC3, DU145, 22Rv1, and LNCaP were plated at different densities in 6-well plates 24 hours before treatment with RK-33, and radiation treatment with different doses was administered 1 hour after adding RK-33. After incubation for 2–3 weeks, colonies were stained with 0.05% (w/v) crystal violet and counted. All experiments were performed in triplicates.

Mice experiments

Animal experiments were conducted in accordance with guidelines from the Johns Hopkins Animal Care and Use Committee. Mice were maintained under pathogen-free conditions with regulated temperature and humidity. Mice were randomly assigned in groups of 5 per cage, and given food and water *ad libitum* under controlled light/dark cycles.

SCID (NCI, Fredrick, MD) mice were purchased (32 in total) at 4–6 weeks of age. DU145-Luc cells in growth medium mixed with Matrigel (1:1; 2.5 million cells per injection) were inoculated in both the right and left flanks of 6- to 8-week-old male SCID mice using a 28-gauge needle, when mice were anesthetized using 3% isoflurane. Mice were monitored weekly until a tumor could be felt by palpation.

Mice were randomly redistributed into four groups of 8 according to their tumor growth, which resulted in an approximately equal distribution of tumor size at the beginning of radiation and RK-33 drug treatment. The four groups of mice were blindly chosen for four different experimental procedures, including control (injection of DMSO only), RK-33 treatment (injection of RK-33 only 50 mg/kg), radiation (one-time radiation of 5 Gy), or radiation and RK-33 treatment (combination of radiation of 5 Gy and RK-33 injection). RK-33 and DMSO were injected intraperitoneally thrice weekly for two weeks. Radiation was performed at the beginning of drug injection using the Small Animal Radiation Research Platform (SARRP; ref. 24) with a circular beam of 1-cm diameter, focusing on the tumor site. Mice of each group were euthanized 0 and 24 hours after radiation and tumors were extracted for γH2AX, cleaved caspase-3, and Ki67 staining. The remaining mice of each group were imaged with a Xenogen IVIS Spectrum (PerkinElmer), with injection of D-luciferin 5 minutes before imaging. Mice were euthanized after 6 weeks of imaging and tumors were extracted for hematoxylin and eosin (H&E) staining, cleaved caspase-3, and Ki67 staining. Morphology of the tumors after RK-33 and radiation treatment was assessed by a veterinary pathologist on H&E-stained sections.

Immunofluorescence

Prostate cancer cells PC3, DU145, and LNCaP (20,000 cells/plate) were allowed to attach overnight in chamber slides. Cells were incubated with RK-33 (PC3 12 μmol/L, DU145 3 μmol/L, LNCaP 6 μmol/L) for 1 hour before 2 Gy radiation treatment. After 0, 1, 6, and 24 hours of radiation, cells were fixed for 15 minutes in 4% formalin, washed with PBS, permeabilized with 0.2% Triton X-100 for 5 minutes, and blocked with 10% goat serum for 30 minutes. Cells were incubated with anti-γH2AX mAb (dilution 1:1,600, EMD Millipore) antibodies in 0.5% BSA/PBS for 1 hour. Next, cells were washed with PBS and incubated with the secondary antibodies, CY3 (dilution 1:200, goat anti-mouse, Jackson ImmunoResearch) for 1 hour. Cells were washed, nuclei-stained with 4′,6-diamidino-2-phenylindole (DAPI), and cover-slipped. Photographs were taken with a Nikon Eclipse 80i fluorescence microscope using a CoolSnap ES camera (Roper Scientific).

Patient samples

Representative paraffin-embedded tissue blocks of 71 prostate cancer patients were taken from the archive of the Department of Pathology of the University Medical Centre in Utrecht (Utrecht, the Netherlands) and routinely processed into a tissue microarray, as described previously (25). The clinicopathologic data, including tumor PSA, Gleason score, tumor stage, lymph node involvement, perineural growth, and resection success, was collected from patient files (Supplementary Table S1). Risk group was determined following EAU/ESTRO guidelines. Protein

expression data by IHC of von Hippel–Lindau tumor suppressor protein (VHL), prolyl hydroxylase domain-containing protein 1 (PHD1), PHD3, VEGF, Glucose transporter 1 (GLUT1), carbonic anhydrase 9 (CA9), Ki67, and the androgen receptor (AR) were derived from previous studies (25). Survival statistics were obtained from the Comprehensive Cancer Centre, the Netherlands (IKNL).

As we used archival leftover pathology material and our study did not affect the included patients, no ethical approval was required according to Dutch legislation (26). Use of anonymous or coded leftover material for scientific purposes is part of the standard treatment contract with patients in the UMCU, congruent with Dutch law (27). Hence, the requirement for consent was waived.

IHC

Four-micron sections were cut, transferred on SuperFrost slides (Menzel & Glaeser), deparaffinized in xylene, and rehydrated in decreasing ethanol dilutions. Endogenous peroxidase was then blocked with 0.3% hydrogen peroxide buffer for 15 minutes for DDX3 and 3% hydrogen peroxide buffer in methanol for 10 minutes for Ki67, γH2AX, and cleaved caspase-3 (CC3). Antigen retrieval was performed by boiling in 10 mmol/L citrate buffer (pH 6.0) for 20 minutes, cooling, and washing with PBS.

Slides were subsequently incubated in a humidified chamber for 1 hour with anti-DDX3 (dilution 1:1,000, polyclonal antibody r647; ref. 21), anti-Ki67 (dilution 1:1,000, Leica Biosystems), or anti-CC3 (dilution 1:1,000, Cell Signaling Technology), or overnight with anti-γH2AX (dilution 1:500, Cell Signaling Technology). Secondary poly-HRP-anti-mouse/rabbit/rat IgG (BrightVision, Immunologic) for 30 minutes was used for DDX3 slides and poly-HRP anti-rabbit IgG (Leica Biosystems) for 1 hour was used for all other stainings. Subsequently, slides were washed with PBS and developed with diaminobenzidine, and lightly counterstained with hematoxylin and mounted. Appropriate positive and negative controls were used throughout.

For mice tumor slides, scoring of Ki67, γH2AX, and CC3 was performed by scoring the percentage of positive nuclei per tumor. For patient tumor slides, the intensity of cytoplasmic DDX3 expression was scored semiquantitatively as absent (0), low (1), moderate (2), or high (3). Cases with score of 0 to 2 were classified as having low DDX3 expression and evaluated against cases with strong expression, as performed previously (8, 19, 28). Nuclear expression of DDX3 was scored as absent or present. Two observers (P.J. van Diest and G.M. Bol) scored the slides, in consensus.

Statistical analysis

All experiments were performed a minimum of three times. Cytotoxicity graphic data were presented as the mean percentages of control ± SEM. Linear regression analysis was used to compute the concentration of test agent needed to reduce mitochondrial activity by 50%, termed the midpoint cytotoxicity. Statistical analyses were carried out with SPSS 23.0 for Windows (IBM Inc.). Only two-sided P values <0.05 were considered significant and are indicated by an asterisk (*) in the figures. Expression levels of DDX3 and the clinicopathologic features were compared by χ^2 test, t test, Fisher exact test, or Mann–Whitney, whenever applicable. Overall survival of prostate cancer patients was assessed by computing Kaplan–Meier curves, and differences between the curves were tested by the log-rank test.

Results

Overexpression of DDX3 correlates to prostate cancer progression

DDX3 overexpression has an oncogenic role in many cancer types including but not limited to breast cancer, lung cancer, medulloblastomas, and colorectal cancer (6, 19, 29, 30). To corroborate our findings in prostate cancer patients, we analyzed a total of 90 samples for DDX3 expression and found that there was a significant difference ($P < 0.02$) in the staining intensity of DDX3 in cancer cells compared with normal cells (Fig. 1A). In addition, prostate cancer samples exhibited a differential cytoplasmic and nuclear staining pattern (Fig. 1A). We also searched the Oncomine database to confirm our results. The Wallace prostate dataset (31) showed that the DDX3 mRNA expression of prostate adenocarcinoma was more than two times higher than that of the normal prostate gland (data not shown). Clinicopathologic characteristics of patients with low and high DDX3 expression can be seen in Supplementary Table S1. No significant correlations were observed between either cytoplasmic or nuclear DDX3 expression or other variables (data not shown). Cytoplasmic DDX3 was associated with other immunohistochemical markers (Supplementary Table S2). A positive correlation was observed with p21 ($P = 0.038$) and AR expression ($P = 0.006$). Cytoplasmic DDX3 correlated positively with cytoplasmic PHD2 ($P = 0.042$), cytoplasmic PHD3 ($P = 0.002$), and cytoplasmic CA9 ($P < 0.001$). Nuclear DDX3 correlated positively with nuclear PHD2 ($P = 0.004$) and negatively with AR ($P = 0.003$) and cytoplasmic VHL ($P = 0.008$).

Follow-up of prostate cancer patients with a low or high cytoplasmic DDX3 expression level indicated that there were no significant differences in patient's survival rate (Fig. 1B and C).

Knockdown of DDX3 in prostate cancer cell lines with various DDX3 expression levels

As overexpression of DDX3 has been related to prostate cancer, we assessed the protein levels of four prostate cancer cell lines, including three androgen-insensitive cell lines (PC3, DU145, and 22Rv1) and one androgen-sensitive cell line (LNCaP). We discovered that the DDX3 expression levels of DU145 and LNCaP were high, while 22Rv1 had moderate expression and PC3 had low expression of DDX3 (Fig. 2A). To assess the function of DDX3 in prostate cancer, we generated DDX3 knockdown cell lines of DU145, PC3, and 22Rv1 (Fig. 2B). Knockdown of DDX3 significantly reduced the clonogenic ability in DU145, partially reduced the clonogenic ability in 22Rv1, but not in PC3, which is characterized by low expression of DDX3 (Fig. 2C). DDX3 knockdown significantly slowed the proliferation rate in DU145 and 22Rv1, but did not affect the proliferation of PC3 (Fig. 2D). We confirmed the specificity of shDDX3 targeting with the help of a rescue experiment (Supplementary Fig. S1).

RK-33 inhibits proliferation of prostate cancer cell lines dependent on DDX3 expression levels and causes cell-cycle arrest

Recently, our laboratory synthesized a small-molecule RK-33 (Fig. 3A), which serves as a DDX3 inhibitor with radiosensitizing properties. RK-33 has anticancer activity in lung cancer, as well as many other cancer types, including breast cancer and sarcoma (16, 17, 19, 32). An MTS (3-(4,5-dimethylthiazol-2-

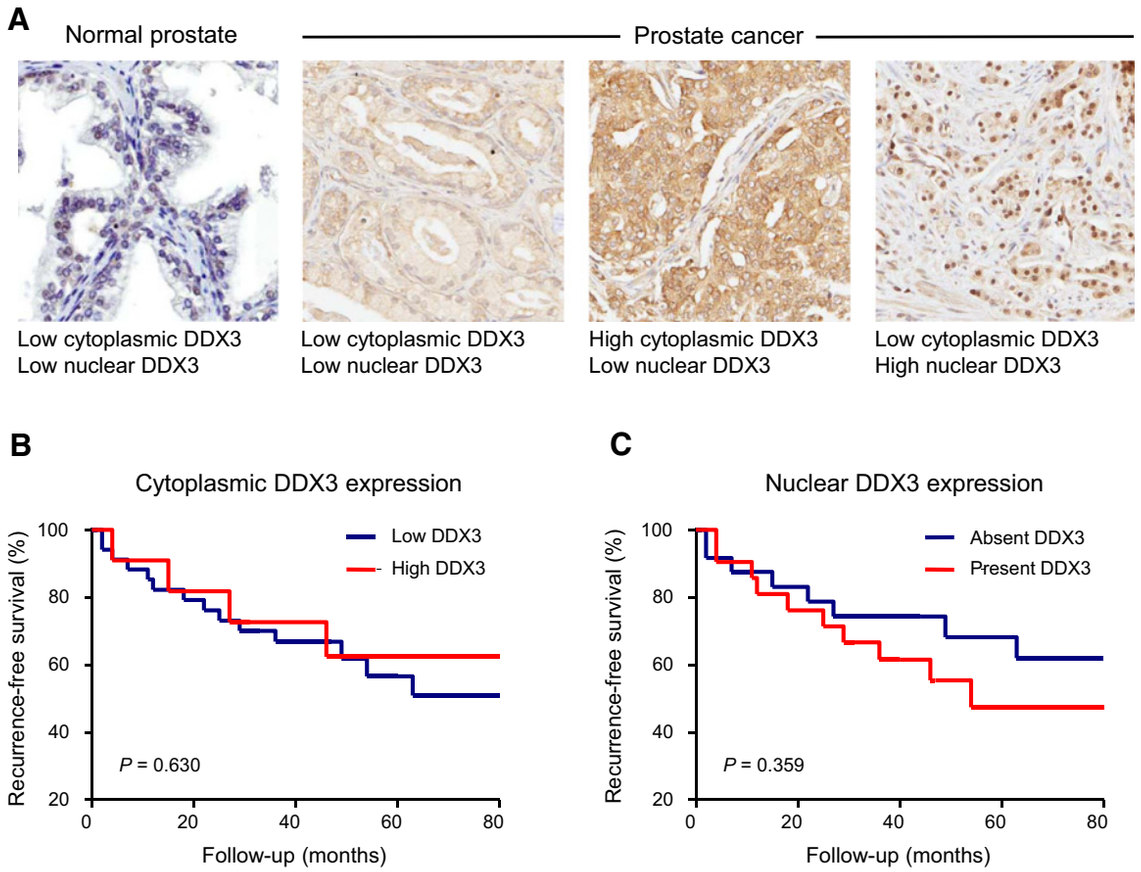

Figure 1.
Correlation of DDX3 expression and prostate cancer. **A,** the staining intensity of DDX3 in normal (left) versus cancer cells (right; Gleason grade 7 or higher) was significant ($P < 0.02$). HA total of 90 samples were stained with DDX3. **B,** survival analysis of prostate cancer patients in low and high cytoplasmic DDX3-expressing tumors. (Kaplan–Meier curve and log-rank test, $P = 0.630$). **C,** survival analysis of prostate cancer patients in absent and present nuclear DDX3-expressing tumors. (Kaplan–Meier curve and log-rank test, $P = 0.359$).

yl)-5-(3-carboxymethoxyphenyl)-2-(4-sulfophenyl)-2H-tetrazolium) assay of RK-33 treatment showed that DU145, LNCaP, and 22Rv1 were sensitive to RK-33 at half-maximal inhibitory concentration (IC_{50} 3–6 μmol/L), whereas PC3 was much less sensitive to RK-33 (IC_{50} >12 μmol/L; Fig. 3B). It is worth noting that DU145, with the highest amount of DDX3 expression levels, showed the most sensitivity to RK-33 treatment, whereas PC3, with the lowest amount of DDX3 expression levels, showed the least sensitivity to RK-33. RK-33 also inhibits DDX3 helicase function, which is involved in translation and cell-cycle regulation (33). To determine whether growth inhibition of prostate cancer cell lines by RK-33 involved cell-cycle arrest, we performed flow cytometry analysis on RK-33–treated cancer cell lines (Fig. 3C). PC3 did not show a significant difference between RK-33–treated and untreated cells, while the cell cycle in DU145, LNCaP, and 22Rv1 cells was perturbed by RK-33 treatment. RK-33 treatment caused a significant accumulation in the G_1 phase for DU145 and LNCaP ($P < 0.05$), although treatment with RK-33 caused only a moderate accumulation of the G_1 phase for 22Rv1, and the treated cells had significantly reduced G_2 phase. In cell lines with a high expression level of DDX3 (DU145 and LNCaP), arrest occurred in the G_1 phase after treatment with RK-33. RK-33 treatment also caused moderate G_1 accumulation in 22Rv1. However, RK-33 did not perturb the cell cycle of PC3, which is characterized by low DDX3 expression levels. Thus, the RK-33 perturbation of the cell cycle in prostate cancer cell lines may be dependent on the expression level of DDX3.

RK-33 reduced cell motility in DU145 and PC3 cell lines

As RK-33 inhibits the proliferation of prostate cancer cell lines and causes G_1 arrest, we next asked whether RK-33 could reduce the motility of prostate cancer cells. We chose PC3 and DU145 for the motility assay as the motility of 22Rv1 itself is low and LNCaP grows slowly and tends to detach after certain confluence. The result of the scratch assay indicated that treatment with RK-33, even at lower concentrations (1.5 μmol/L for DU145 and 6 μmol/L for PC3), reduced the motility for migration compared with untreated prostate cancer cells of DU145 and PC3, in which the scratch gaps were completely filled in 36 hours (Supplementary Figs. S2 and S3). Moreover, the higher concentration of RK-33 reduced the cancer cell motility more than the lower concentration. We confirmed these results with the help of a Boyden chamber assay (Supplementary Fig. S4).

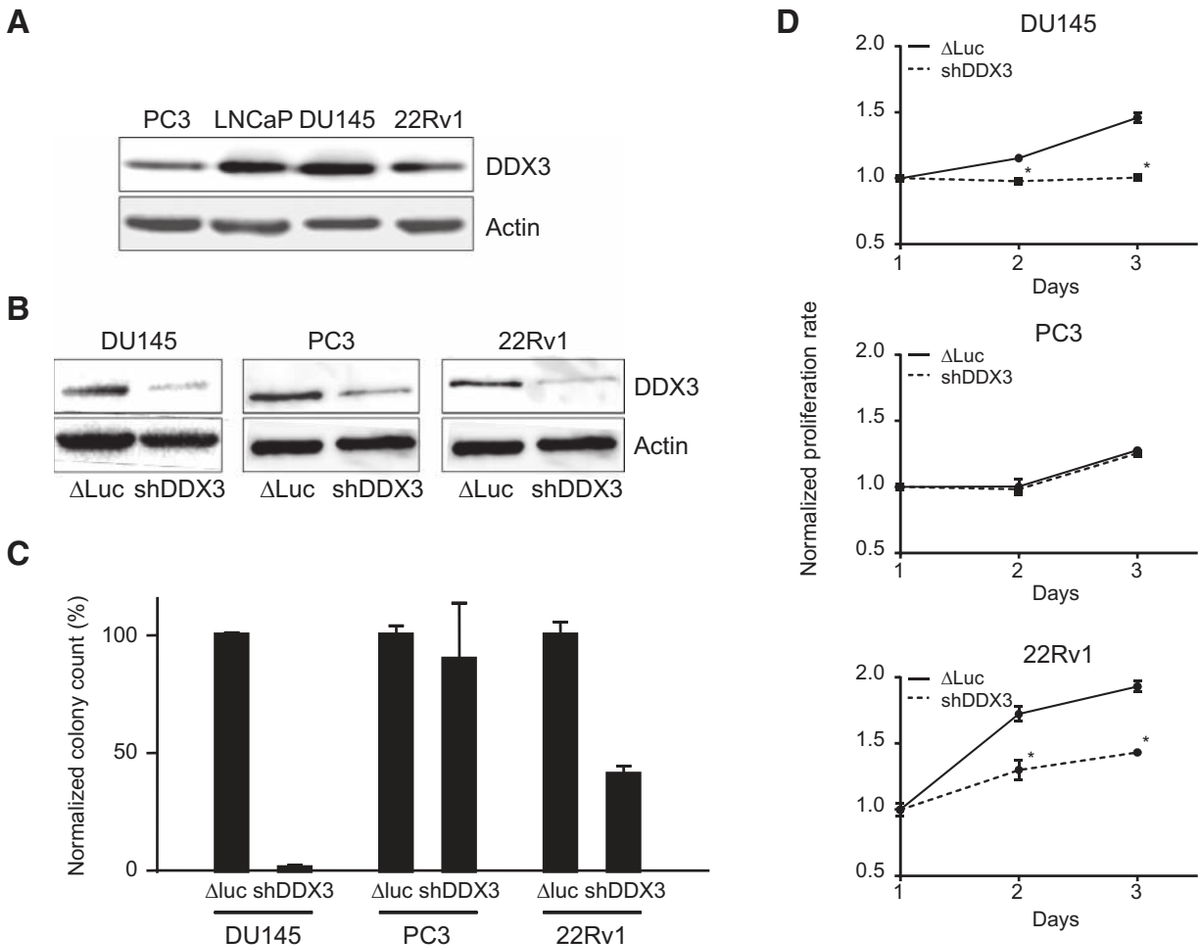

Figure 2.

The effect of DDX3 knockdown on prostate cancer colony-forming ability and cell proliferation rate. **A,** DDX3 expression level of prostate cancer cell lines including PC3, LNCaP, DU145, 22Rv1. **B,** immunoblot indicating DDX3 knockdown by shDDX3 lentiviral vector. **C,** normalized colony counts of prostate cancer cell lines DU145, PC3, 22Rv1 transduced with control vector and shDDX3 lentiviral vector, respectively. **D,** normalized proliferation rate of prostate cancer cell lines DU145, PC3, 22Rv1 transduced with control vector and shDDX3 lentiviral vector.

Combination of RK-33 and radiation reduced clonogenicity in a synergistic or additive pattern

As radiotherapy is one of the major treatment options for prostate cancer patients and RK-33 has been identified as a radiosensitizer for lung cancer (18, 19), we explored the treatment combination of radiation and RK-33 for the clonogenicity of prostate cancer cells, including PC3, DU145, 22Rv1, and LNCaP. In this experiment, we chose different radiation doses according to the sensitivity of the prostate cancer cells. The results indicated that the treatment combination of RK-33 and radiation exhibited a synergistic effect in DU145 and LNCaP cells that overexpress DDX3 (Fig. 4). In contrast, 22Rv1 and PC3, with lower DDX3 expression, showed lower RK-33–induced radiosensitization. In this combination study, we used the Bliss Independence Model (34) as we made the assumption that radiation and RK-33 act independently to inhibit the proliferation of cancer cells. As described earlier, the effect of RK-33 alone was normalized; therefore, the overlapping curves for radiation alone and the combination of RK-33 and radiation indicated an additive effect in PC3 cells. The survival curve of the combination, which was below that of radiation alone, indicated a synergistic effect in 22Rv1, DU145, and LNCaP (Fig. 4).

Immunocytochemistry of γH2AX indicates a slowed DNA damage repair process in cells treated with a combination of RK-33 and radiation

As radiation causes DNA double-strand breaks in cancer cells, the cancer cells recruit DNA damage repair proteins to help survive after radiation. γH2AX, the phosphorylated form of the histone H2AX, is the first step in recruiting and localizing DNA repair protein (35). To explore the possible mechanism of the synergistic effect of the treatment combination of RK-33 and radiation, we investigated the marker of DNA double-strand breaks, γH2AX, in the three prostate cancer cell lines, PC3, DU145, and LNCaP. The result shown in Fig. 5 indicated that γH2AX foci increased dramatically 1 hour after radiation and gradually fell after the double-strand breaks were repaired. Compared with radiation treatment alone, the combination

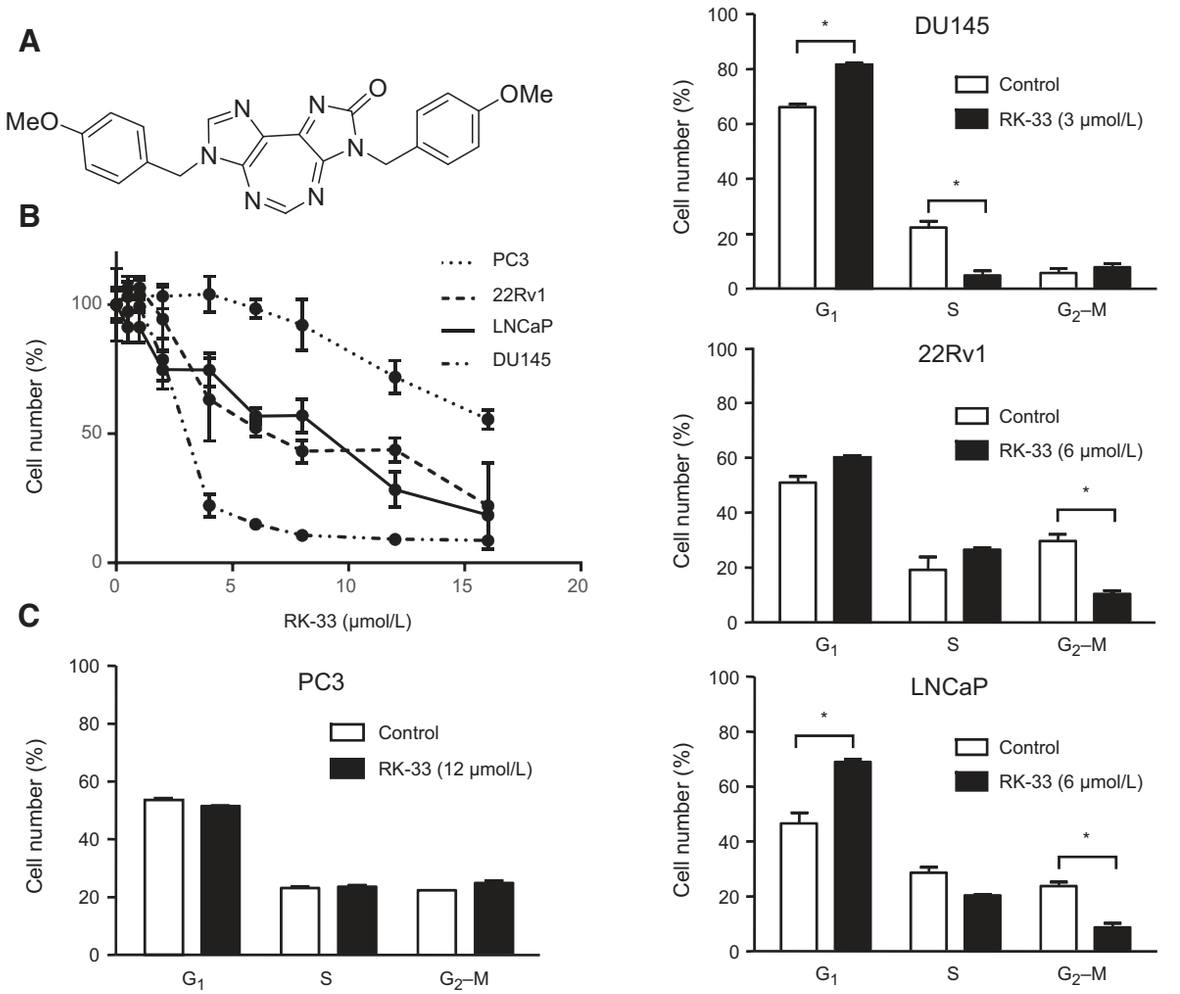

Figure 3.

The effect of RK-33 on cell viability and cell-cycle control of prostate cancer cell lines including PC3, DU145, 22Rv1 and LNCaP. **A,** the structure of small DDX3 inhibitor RK-33. **B,** cell viability assay of RK-33 on PC3, DU145, 22Rv1, and LNCaP. **C,** cell-cycle analysis by flow cytometry of RK-33 on prostate cancer cell lines PC3, DU145, 22Rv1, and LNCaP.

treatment did not result in more double-strand breaks at 1 hour for DU145; however, there were more foci at 6 and 24 hours. In LNCaP cells, there were more γH2AX foci even at 1 hour. In PC3 cells, only at 24 hours were there more foci in the treatment combination of RK-33 and radiation. This is an indicator that the DNA damage repair process in the presence of RK-33 has been slowed or requires more γH2AX to overcome the inhibition of DNA damage repair by caused by RK-33.

In vivo combination treatment of RK-33 and radiation in DU145-luc SCID mice

The promising results of the treatment combination of RK-33 and radiation *in vitro* encouraged us to explore the combination treatment in a mouse model. Four randomized groups of SCID mice inoculated with DU145-Luc (engineered with luciferase) were treated with DMSO, RK-33, and the combination of RK-33 and radiation, and tumors were imaged for bioluminescence emission. As shown in Fig. 6A, tumors of the DMSO and RK-33 groups weighed more than those of the radiation and RK-33 radiation groups. The median weight of tumors in the DMSO group was slightly higher than that in the RK-33 group. There was no significant difference in median weight for the radiation and RK-33 radiation group (median weight between 30 and 40 mg). As the sizes of tumors treated with radiation or radiation combined with RK-33 were small, measuring tumor weight or tumor size may not have accurately reflected tumor growth or tumor necrosis. We used luciferase-engineered DU145 cells for bioluminescence imaging on an IVIS system, which is more sensitive and accurate for the early detection of tumor growth and development, tumor cell death, and necrosis (36, 37). The signal we detected, total flux, is proportional to the number of light-emitting cells and the calibrated IVIS system allowed us to monitor tumor growth more accurately and over a long period of time. The imaging results indicated that the tumor growth of the radiation group was significantly higher compared with the combination group. Tumor growth in the radiation group

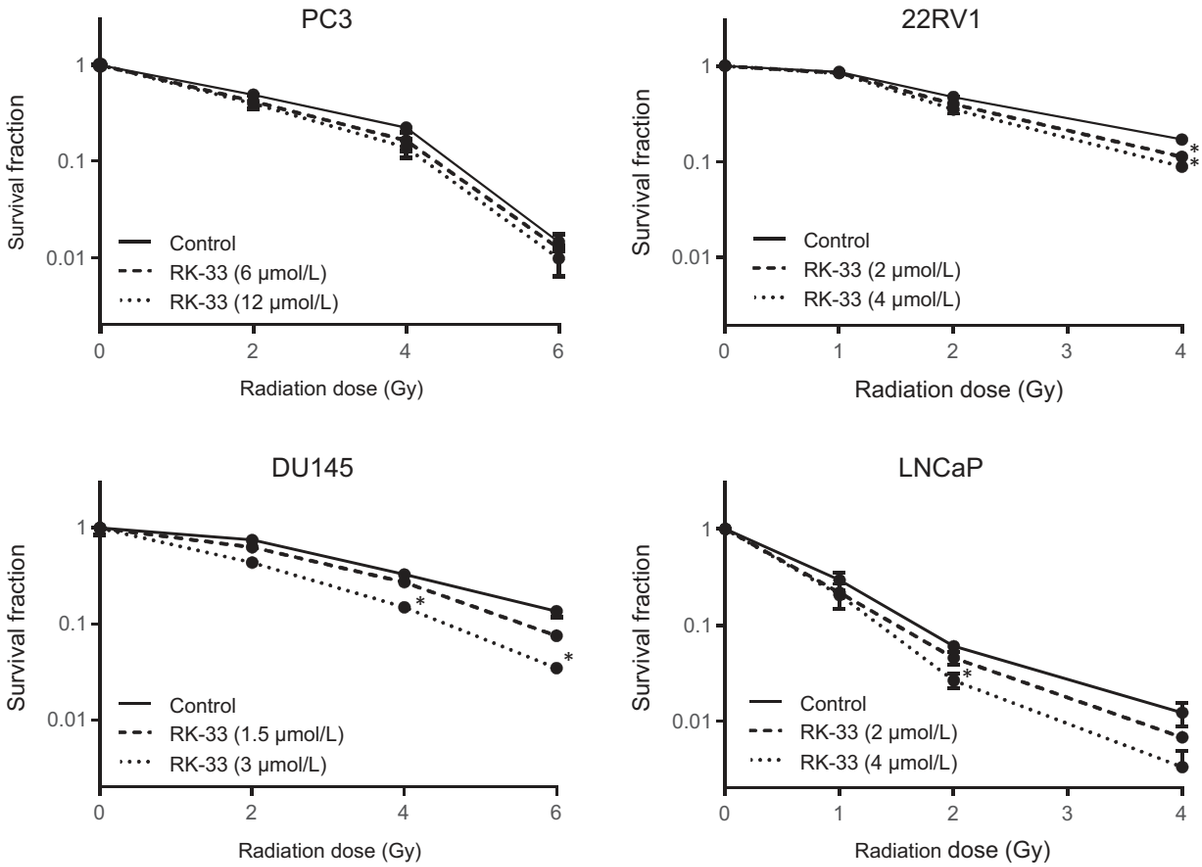

Figure 4.
Combination effect of RK-33 treatment and radiation on colony formation of prostate cancer cell lines including PC3, DU145, 22Rv1, and LNCaP.

increased significantly over 5 weeks of measurement, while tumor growth in the combination group did not increase at all after the second week (Fig. 6B). To study the differential tumor growth in the two groups, tumors from dissected mice were sliced and stained with Ki67 and cleaved caspase-3 antibody. As shown in Fig. 6C, there were less cells stained with Ki67 antibody and more cells stained with cleaved caspase-3 antibody in the tumors of the combination group, indicating less proliferation and more apoptosis. The representative pictures of cleaved caspase-3 and Ki67 staining are shown in Fig. 6D. H&E staining indicated that there was more cell death (pyknotic or condensed nuclei) admixed with fibrin and interstitial edema in the tumors from mice from the combination RK-33 and radiation group compared with the control or single treatment groups (Fig. 6E).

To determine whether the DNA damage repair pathway was disturbed by the combination of RK-33 and radiation, a subset of mice inoculated with DU145-Luc were randomly divided into four groups for DMSO, RK-33, radiation, and the combination of RK-33 and radiation. Mice were dissected at 30 minutes and 24 hours after radiation treatment. Tumor sections were stained with γH2AX, Ki67, and cleaved caspase-3 antibody. γH2AX levels increased even at 30 minutes after radiation and γH2AX levels remained high at 24 hours after radiation for the combination treatment, while γH2AX levels decreased more than 60% at 24 hours for the radiation group (Supplementary Fig. S5). These results confirmed our *in vitro* findings. The results of Ki67 and cleaved caspase-3 indicated that radiation treatment (both radiation and the combined treatment of radiation and RK-33) decreased Ki67 levels and increased cleaved caspase levels at 30 minutes of radiation, and the effects of radiation for Ki67 and cleaved caspase-3 were sustained for at least 24 hours. RK-33 treatment alone did not affect the tumor proliferation at either time point (Ki67 levels equal to DMSO group), but did induce apoptosis at 24 hours after treatment (cleaved caspase-3 level increased at 24 hours). Thus, the treatment combination of RK-33 and radiation has an advantage in reducing tumor proliferation, possibly through inhibiting the DNA damage repair pathway by RK-33.

Discussion

Prostate cancer, sometimes viewed as a chronic and manageable disease, still remains the most prevalent cancer and second leading cause of cancer-related deaths in males in the United States. The current treatment armamentarium for prostate cancer includes surgery, radiation, hormonal therapy, cytotoxic chemotherapy, and immunotherapy. The major chemotherapy drugs effective for locally advanced and metastatic

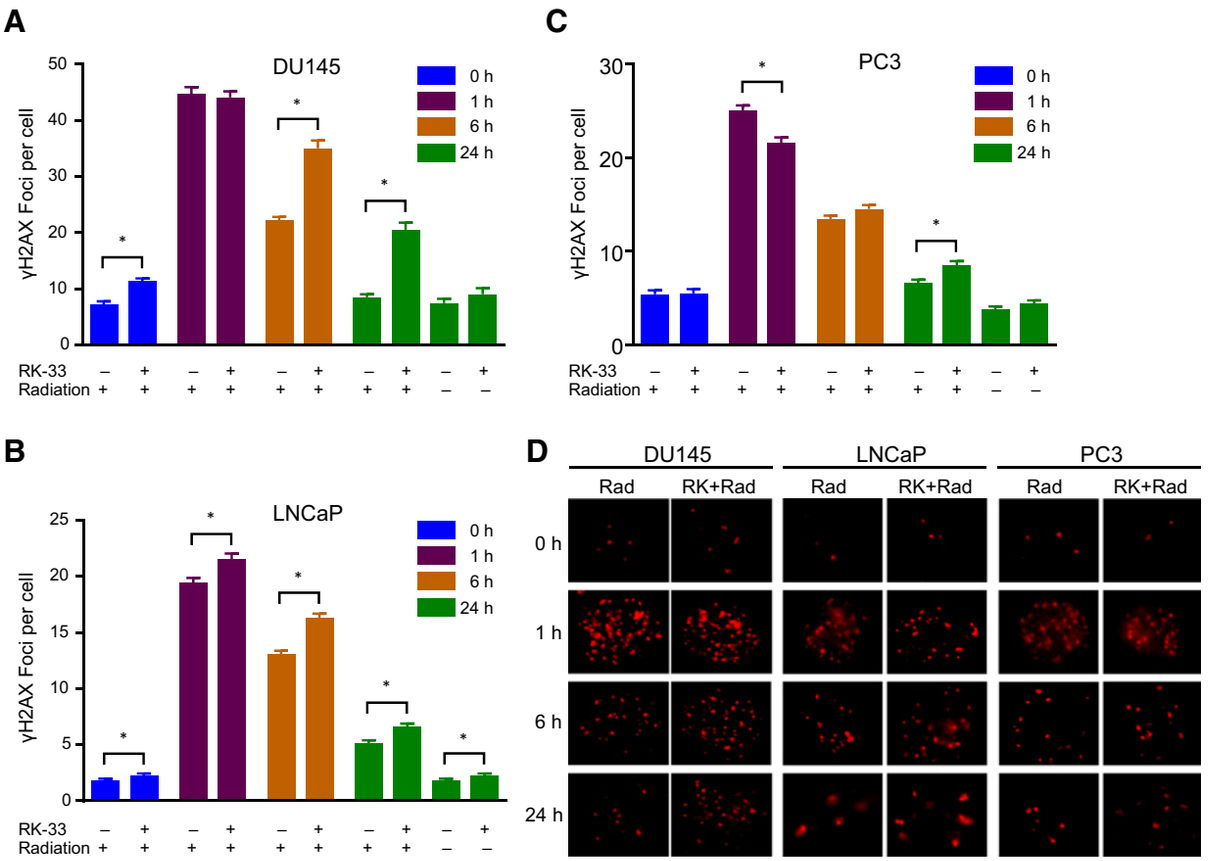

Figure 5.

Effect of RK-33 treatment on radiation-induced DNA damage represented by γH2AX foci. **A,** DU145 cells (20,000 cells per chamber slide) treated with 3 μmol/L RK-33/2 Gy radiation; γH2AX foci per cell were counted for treatment as indicated in the graph. **B,** LNCaP cells (20,000 cells per chamber slide) treated with 6 μmol/L RK-33/2 Gy radiation. **C,** PC3 cells (20,000 cells per chamber slide) treated with 12 μmol/L RK-33/2 Gy radiation. **D,** representative γH2AX foci pictures for three prostate cancer cell lines (DU145, PC3, and LNCaP) with radiation or combination treatment of radiation and RK-33 at time 0, 1, 6, and 24 hours.

prostate cancer are the taxanes, which disrupt microtubule function. In addition, radiotherapy is a well-established treatment for localized and locally advanced prostate cancer, but radiation efficacy for poor-risk disease still requires improvement. Physical radiation dose escalation has reached a maximum secondary to dose-limiting rectal and genitourinary toxicity. Another approach to increase the efficacy of radiotherapy are via tumor-specific radiosensitizing agents. Thus, alternate strategies and drugs with new mechanisms of action are needed in the prostate cancer field.

DDX3 has been discovered to play an oncogenic role in tumorigenesis in many cancer types, including breast cancer, lung cancer, medulloblastoma, and colorectal cancer (6, 19, 29, 30, 38). Although there are some controversial data indicating that DDX3 is a tumor suppressor (39–41), it is possible that the function of DDX3 is organ-specific. Our previous data in lung cancer indicate that inhibition of DDX3 function by a small-molecule inhibitor, RK-33, reduces cell proliferation in lung cancer and radiosensitizes lung cancer cells in a DDX3-dependent manner (19). Radiotherapy remains one of the mainstays for prostate cancer treatment, making DDX3 inhibition a highly promising therapeutic approach. RK-33, as a nontoxic small molecule, which inhibits DNA repair induced by radiation, would be a promising option for a combination radiation treatment for prostate cancer.

Our clinical data indicate that prostate cancer patients express higher DDX3 levels compared with normal patients. Also, distinct nuclear and cytoplasmic DDX3 expression was observed in some prostate cancer patient samples. It is possible that the presence of nuclear DDX3 corresponds with altered translational demands in cancers, but the exact role of nuclear versus cytoplasmic DDX3 remains to be elucidated. Also, the differential localization of DDX3 within the cancer cells may reflect the multifunctional role of DDX3 not only in translation but also enhancing specific transcriptional products and regulating discrete cellular processes. Through searching Oncomine database, we also found that the DDX3 mRNA expression level is higher in prostate adenocarcinoma. To determine DDX3 function in prostate cancer cell lines, we have knocked down DDX3 in three prostate cancer cell lines (PC3, DU145, and 22Rv1) and found that DDX3 knockdown reduces cell proliferation and clonogenicity in DU145 and 22Rv1, but not in PC3. We checked the DDX3 levels of four prostate cancer cell lines (PC3, DU145, 22Rv1, and LNCaP) and found that

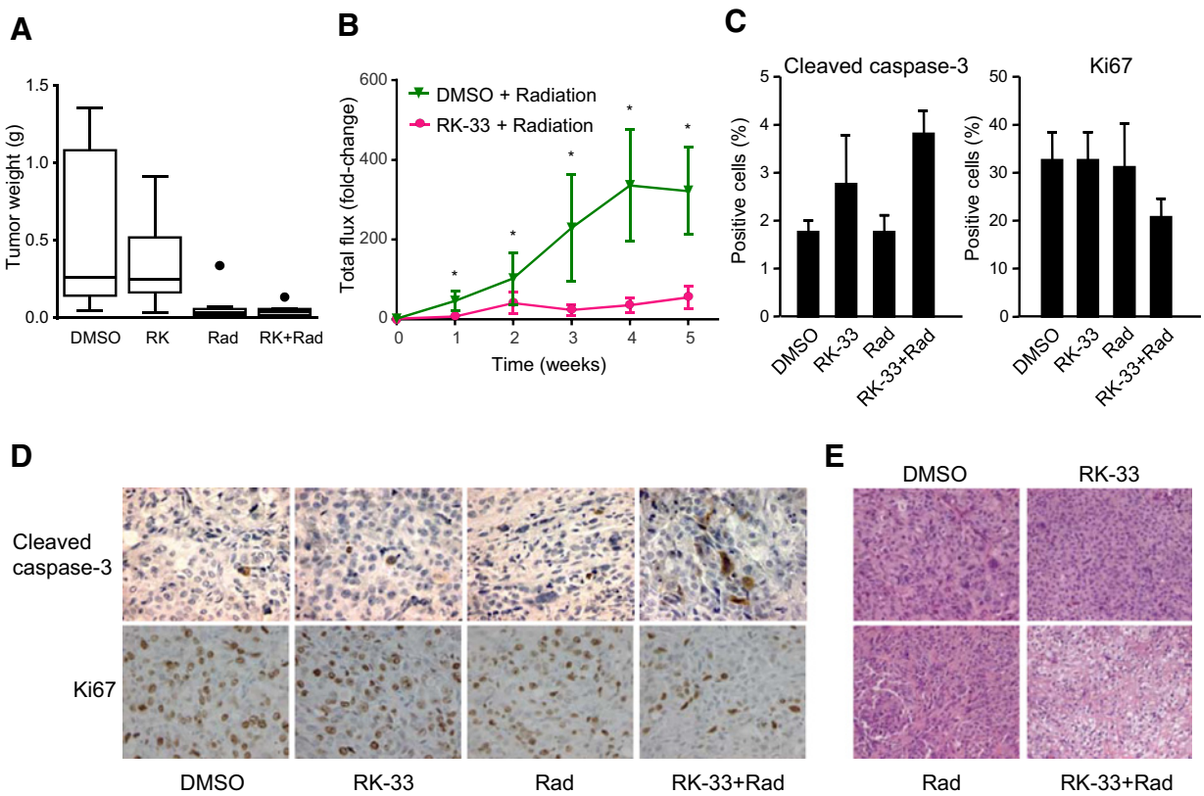

Figure 6.

Combination treatment in DU145-Luc–inoculated SCID mice reduced tumor growth. **A,** box plot of tumor weight of four mice groups treated with DMSO, RK-33, radiation, and combination of RK-33 and radiation. **B,** tumor growth rate of radiation normalized to week 0 indicated by fold change of total flux of bioluminescence emission from live DU145-Luc–inoculated tumors. **C,** bar graph indicating percentage of nuclei positive for Ki67 (left) and cleaved caspase-3 (right) per tumor per treatment group. **D,** example of cleaved caspase-3 expression (top) and Ki67 expression (bottom) of each treatment group at ×40 magnification. **E,** H&E staining of tumor slides of each treatment group. Tumors were analyzed 5 weeks after treatment.

DU145 and LNCaP overexpressed DDX3, 22Rv1 expressed moderate levels of DDX3, whereas PC3 expressed low levels of DDX3. The low expression level of DDX3 in PC3 may indicate that the role of DDX3 is not as crucial in PC3 cell lines as in other cell lines. RK-33 treatment of four prostate cancer cell lines indicated that the efficiency of RK-33 in inhibiting cell proliferation could be related to the DDX3 expression levels. Cell-cycle analysis of prostate cancer cell lines indicates that RK-33 causes cell-cycle arrest at the G_1 phase. The wound-healing assay (scratch assay) of PC3 and DU145 treated with RK-33 indicates that RK-33 reduced cell motility in DU145 and even in PC3.

RK-33, being a nontoxic drug *in vivo*, would be an ideal radiosensitizer in combination with radiation treatment in prostate cancer, and will have a benefit by reducing radiation dose and frequency, while maintaining or improving upon tumor cell kill. To assess whether the combination of RK-33 and radiation was synergistic, an *in vitro* clonogenic assay and an *in vivo* imaging of mice inoculated with DU145-Luc were performed. The combination of RK-33 and radiation reduced colony-forming ability significantly in DU145 and LNCaP, but only slightly in 22Rv1 and PC3. Combination of 3 μmol/L RK-33 and 6 Gy radiation for DU145 and a combination of 6 μmol/L RK-33 and 4 Gy radiation for LNCaP reduced clonogenic ability two to three times more compared with radiation treatment alone, while the combination of 6 μmol/L RK-33 and 4 Gy radiation for 22Rv1 and the combination of 12 μmol/L RK-33 and 6 Gy radiation reduced clonogenic ability 50%–100% more compared with radiation treatment alone. The *in vivo* combination treatment of RK-33 and radiation caused less tumor cell proliferation and more cell apoptosis in the DU145-Luc–inoculated SCID mice model. Both *in vitro* and *in vivo* immunostaining indicated that the DNA damage repair process in DDX3-rich cell lines (DU145 and LNCaP *in vitro*, DU145 *in vivo*) were slowed by the treatment combination of RK-33 and radiation, which may explain the synergistic effect of the combination treatment in reducing the clonogenicity and proliferation rate, as well as inducing apoptosis in prostate cell lines.

In conclusion, DDX3 could serve as a marker of high grade and aggressive prostate cancer and the small-molecule DDX3 inhibitor, RK-33, could function as a radiosensitizer for prostate cancers with a high DDX3 expression.

Disclosure of Potential Conflicts of Interest

V. Raman, P.J. van Diest, and G.M. Bol have ownership interest (including patents) as a co-owner of a patent on DDX3 targeting. No potential conflicts of interest were disclosed by the other authors.

Authors' Contributions

Conception and design: M. Xie, F. Vesuna, G.M. Bol, V. Raman
Development of methodology: M. Xie, F. Vesuna, G.M. Bol, P.J. van Diest, V. Raman
Acquisition of data (provided animals, acquired and managed patients, provided facilities, etc.): M. Xie, F. Vesuna, G.M. Bol, M.R.H. van Voss, K. Nugent, R. Malek, P.J. van Diest, P.T. Tran, V. Raman
Analysis and interpretation of data (e.g., statistical analysis, biostatistics, computational analysis): M. Xie, F. Vesuna, G.M. Bol, M.R.H. van Voss, P.J. van Diest, V. Raman
Writing, review, and/or revision of the manuscript: M. Xie, F. Vesuna, G.M. Bol, M.R.H. van Voss, P.J. van Diest, P.T. Tran, V. Raman
Administrative, technical, or material support (i.e., reporting or organizing data, constructing databases): M. Xie, F. Vesuna, P.J. van Diest, P.T. Tran, V. Raman
Study supervision: F. Vesuna, V. Raman
Other (performed experiments): S. Tantravedi

Grant Support

This work was supported by the Patrick C. Walsh Prostate Cancer Research Fund (V. Raman).

The costs of publication of this article were defrayed in part by the payment of page charges. This article must therefore be hereby marked *advertisement* in accordance with 18 U.S.C. Section 1734 solely to indicate this fact.

Received February 17, 2016; revised August 6, 2016; accepted August 21, 2016; published OnlineFirst September 12, 2016.

References

1. Siegel RL, Miller KD, Jemal A. Cancer statistics, 2016. CA Cancer J Clin 2016;66:7–30.
2. Abate-Shen C, Shen MM. Molecular genetics of prostate cancer. Genes Dev 2000;14:2410–34.
3. Loeb S, Catalona WJ. The Prostate Health Index: a new test for the detection of prostate cancer. Ther Adv Urol 2014;6:74–7.
4. Tran PT, Hales RK, Zeng J, Aziz K, Salih T, Gajula RP, et al. Tissue biomarkers for prostate cancer radiation therapy. Curr Mol Med 2012; 12:772–87.
5. Esfahani M, Ataei N, Panjehpour M. Biomarkers for evaluation of prostate cancer prognosis. Asian Pac J Cancer Prev 2015;16:2601–11.
6. Botlagunta M, Vesuna F, Mironchik Y, Raman A, Lisok A, Winnard P Jr, et al. Oncogenic role of DDX3 in breast cancer biogenesis. Oncogene 2008;27: 3912–22.
7. Chen HH, Yu HI, Cho WC, Tarn WY. DDX3 modulates cell adhesion and motility and cancer cell metastasis via Rac1-mediated signaling pathway. Oncogene 2015;34:2790–800.
8. Bol GM, Raman V, van der Groep P, Vermeulen JF, Patel AH, van der Wall E, et al. Expression of the RNA helicase DDX3 and the hypoxia response in breast cancer. PLoS ONE 2013;8:e63548.
9. Fuller-Pace FV. DExD/H box RNA helicases: multifunctional proteins with important roles in transcriptional regulation. Nucleic Acids Res 2006;34: 4206–15.
10. Abdelhaleem M, Maltais L, Wain H. The human DDX and DHX gene families of putative RNA helicases. Genomics 2003;81:618–22.
11. Linder P, Fuller-Pace F. Happy birthday: 25 years of DEAD-box proteins. Methods Mol Biol 2015;1259:17–33.
12. Rosner A, Rinkevich B. The DDX3 subfamily of the DEAD box helicases: divergent roles as unveiled by studying different organisms and *in vitro* assays. Curr Med Chem 2007;14:2517–25.
13. Soto-Rifo R, Ohlmann T. The role of the DEAD-box RNA helicase DDX3 in mRNA metabolism. Wiley Interdiscip Rev RNA 2013;4: 369–85.
14. Schroder M. Human DEAD-box protein 3 has multiple functions in gene regulation and cell cycle control and is a prime target for viral manipulation. Biochem Pharmacol 2009;79:297–306.
15. Fuller-Pace FV. DEAD box RNA helicase functions in cancer. RNA Biol 2013;10:121–32.
16. Kondaskar A, Kondaskar S, Fishbein JC, Carter-Cooper BA, Lapidus RG, Sadowska M, et al. Structure-based drug design and potent anti-cancer activity of tricyclic 5:7:5-fused diimidazo[4,5-d:4′,5′-f][1,3]diazepines. Bioorg Med Chem 2013;21:618–31.
17. Kondaskar A, Kondaskar S, Kumar R, Fishbein JC, Muvarak N, Lapidus RG, et al. Novel, broad spectrum anti-cancer agents containing the tricyclic 5:7:5-fused diimidazodiazepine ring system. ACS Med Chem Lett 2010; 2:252–56.
18. Bol GM, Xie M, Raman V. DDX3, a potential target for cancer treatment. Mol Cancer 2015;14:188.
19. Bol GM, Vesuna F, Xie M, Zeng J, Aziz K, Gandhi N, et al. Targeting DDX3 with a small molecule inhibitor for lung cancer therapy. EMBO Mol Med 2015;7:648–69.
20. Crook JM, Perry GA, Robertson S, Esche BA. Routine prostate biopsies following radiotherapy for prostate cancer: results for 226 patients. Urology 1995;45:624–31.
21. Angus AG, Dalrymple D, Boulant S, McGivern DR, Clayton RF, Scott MJ, et al. Requirement of cellular DDX3 for hepatitis C virus replication is unrelated to its interaction with the viral core protein. J Gen Virol 2010;91:122–32.
22. Vesuna F, Lisok A, Kimble B, Domek J, Kato Y, van der Groep P, et al. Twist contributes to hormone resistance in breast cancer by downregulating estrogen receptor alpha. Oncogene 2011;31:3223–34.
23. Xie M, Vesuna F, Botlagunta M, Bol GM, Irving A, Bergman Y, et al. NZ51, a ring-expanded nucleoside analog, inhibits motility and viability of breast cancer cells by targeting the RNA helicase DDX3. Oncotarget 2015;6: 29901–13.
24. Wong J, Armour E, Kazanzides P, Iordachita I, Tryggestad E, Deng H, et al. High-resolution, small animal radiation research platform with x-ray tomographic guidance capabilities. Int J Radiat Oncol Biol Phys 2008; 71:1591–9.
25. Jans J, van Dijk JH, van Schelven S, van der Groep P, Willems SH, Jonges TN, et al. Expression and localization of hypoxia proteins in prostate cancer: prognostic implications after radical prostatectomy. Urology 2010;75: 786–92.
26. The Medical Research Involving Human Subjects Act (Wet medisch-wetenschappelijk onderzoek met mensen, WMO; text in Dutch). Burgerlijk wetboek 1998.
27. van Diest PJ. For and against: no consent should be needed for using leftover body material for scientific purposes * For * Against. BMJ 2002; 325:648–51.
28. Heerma van Voss MR, van Kempen PM, Noorlag R, van Diest PJ, Willems SM, Raman V. DDX3 has divergent roles in head and neck squamous cell carcinomas in smoking versus non-smoking patients. Oral Dis 2015; 21:270–1.
29. Robinson G, Parker M, Kranenburg TA, Lu C, Chen X, Ding L, et al. Novel mutations target distinct subgroups of medulloblastoma. Nature 2012; 488:43–8.
30. Heerma van Voss MR, Vesuna F, Trumpi K, Brilliant J, Berlinicke C, de Leng W, et al. Identification of the DEAD box RNA helicase DDX3 as a therapeutic target in colorectal cancer. Oncotarget 2015;6: 28312–26.
31. Wallace TA, Prueitt RL, Yi M, Howe TM, Gillespie JW, Yfantis HG, et al. Tumor immunobiological differences in prostate cancer between African-American and European-American men. Cancer Res 2008;68: 927–36.
32. Wilky BA, Kim C, McCarty G, Montgomery EA, Kammers K, DeVine LR, et al. RNA helicase DDX3: a novel therapeutic target in Ewing sarcoma. Oncogene 2016;35:2574–83.
33. Ariumi Y. Multiple functions of DDX3 RNA helicase in gene regulation, tumorigenesis, and viral infection. Front Genet 2014;5:423.
34. Zhao W, Sachsenmeier K, Zhang L, Sult E, Hollingsworth RE, Yang H. A New Bliss Independence Model to Analyze Drug Combination Data. J Biomol Screen 2014;19:817–21.

35. Kuo LJ, Yang LX. Gamma-H2AX - a novel biomarker for DNA double-strand breaks. In vivo 2008;22:305–9.
36. Lim E, Modi KD, Kim J. In vivo bioluminescent imaging of mammary tumors using IVIS spectrum. J Visual Exp 2009;26:pii:1210.
37. Kocher B, Piwnica-Worms D. Illuminating cancer systems with genetically engineered mouse models and coupled luciferase reporters in vivo. Cancer Discov 2013;3:616–29.
38. Xie M, Vesuna F, Botlagunta M, Bol GM, Irving A, Bergman Y, et al. NZ51, a ring-expanded nucleoside analog, inhibits motility and viability of breast cancer cells by targeting the RNA helicase DDX3. Oncotarget 2015;6: 29901–13.
39. Su CY, Lin TC, Lin YF, Chen MH, Lee CH, Wang HY, et al. DDX3 as a strongest prognosis marker and its downregulation promotes metastasis in colorectal cancer. Oncotarget 2015;6:18602–12.
40. Chao CH, Chen CM, Cheng PL, Shih JW, Tsou AP, Lee YH. DDX3, a DEAD box RNA helicase with tumor growth-suppressive property and transcriptional regulation activity of the p21waf1/cip1 promoter, is a candidate tumor suppressor. Cancer Res 2006;66:6579–88.
41. Wu DW, Lee MC, Wang J, Chen CY, Cheng YW, Lee H. DDX3 loss by p53 inactivation promotes tumor malignancy via the MDM2/Slug/E-cadherin pathway and poor patient outcome in non-small-cell lung cancer. Oncogene 2014;33:1515–26.